2024 IEEE International Conference on Robotics and Automation (ICRA 2024)
May 13-17, 2024. Yokohama, Japan

Design and Implementation of a Robotic Testbench for Analyzing Pincer Grip Execution in Human Specimen Hands

Nikolas Wilhelm[1,2], Claudio Glowalla[1], Sami Haddadin[2], Julian Schote[1], Hannes Höppner[4], Patrick van der Smagt[3,†], Maximilian Karl[3,†] and Rainer Burgkart[1,†]

***Abstract*— This study presents an innovative test rig engineered to explore the kinematic and viscoelastic characteristics of human specimen hands. The rig features eight force-controlled motors linked to muscle tendons, enabling precise stimulation of hand specimens. Hand movements are monitored through an optical tracking system, while a force-torque sensor quantifies the resultant fingertip loads. Employing this setup, we successfully demonstrated a pincer grip using a cadaver hand and measured both muscle forces and grip strength. Our results reveal a nonlinear relationship between tendon forces and grip strength, which can be modeled by an exponential fit. This investigation serves as a nexus between biomechanical and robotics-focused research, providing critical insights for the advancement of robotic hand actuation and therapeutic interventions.**

I. Introduction

The human hand, with its structural complexity and versatility, serves as a central tool for interacting with our environment. The precise coordination of multiple muscles, even for the operation of a single finger, results in movements that are influenced by the viscoelastic properties of ligaments and surrounding tissues, as well as the kinematics of the joints [1], [2], [3].

Numerous hand models have been developed to encapsulate this complexity and simulate the biomechanical behavior of the hand [4], [5], [6]. These models largely rely on Computer Aided Design (CAD) data, supplemented with muscle tractions and hand kinematics. Yet, despite their geometric sophistication, many of these models fall short in comprehensive biomechanical validation. The verification of their outcomes becomes particularly challenging given the intertwined nature of hand modeling systems and the imperative to ascertain a myriad of boundary conditions.

One particular challenge in hand modeling is the thumb, which has been reported to be difficult to model accurately due to its unique joint structure [7]. This has led to the development of new modeling approaches that consider the contacting surfaces and stabilizing tissues of the thumb joint, modeling it as a multi-body system driven by forces exerted by the cartilage contact, ligaments, and muscles [7].

Robotic hand actuation has advanced from basic grippers to complex systems incorporating computer vision, tactile feedback, and computational strategies, as highlighted by Billard and Kragic [8]. Significant achievements include biomimetic hands for limb regeneration [9] and under-actuated designs by Mitsui, Ozawa, and Kou [10], indicating progress towards more adaptable manipulators. Additionally, soft grippers inspired by the Fin Ray® Effect [11] underscore rapid advancements. Moving beyond traditional grip-focused robotics, our research explores human hand biomechanics to bridge robotics and biomechanics, offering a deeper understanding of hand mechanics and setting our work apart from conventional approaches.

Previous experimental setups have explored various aspects of hand behavior. Some have studied finger extension by determining the contact forces of the phalanges through optical tracking and a force plate system [12], while others have incorporated electromyographical signals of the muscles to compare model and tracking outcomes for living patients [13]. Cadaver studies have also been conducted, with one focusing on the movement of the index finger's joints when individual muscles are actuated [14], and another investigating the force exerted during grasping [15]. However, these studies were limited in their scope, often focusing on a single finger and failing to fully correlate muscle activation with movement and exerted force.

In this paper, we present a comprehensive testbed that addresses these limitations. Our system links force-controlled tendon actuation to movement and exerted force at the fingertip. With the capability of controlling eight independent motors, it allows for the examination of more than one finger at a time, enabling the simulation of clinically relevant everyday grasping tasks.

We focus on the pincer grip, a critical fine motor movement used to grasp small objects, where the flexed thumb and index finger come into contact [16]. This grip, learned by infants in their first year of life, represents the pinnacle of fine motor movement achievable by a gorilla [17], [18]. Our experimental setup simulates the pincer grip on a human specimen by controlling four tendons each of the thumb and index finger. In summary, the main contributions of this paper are as follows:

*This work was supported by the "Deutsche Forschungsgemeinschaft (DFG)" within theinterdisciplinary project (BU 1154/8-1, Projektnummer 276036034)

[1]Nikolas Wilhelm, Claudio Glowalla, Julian Schote and Rainer Burgkart are with the Department of Orthopedics and Sports Orthopedics, Klinikum rechts der Isar, School of Medicine, 81675 Munich, Germany

[2]Nikolas Wilhelm and Sami Haddadin are with the Munich Institute of Robotics and Machine Intelligence, Technical University of Munich, 80992 Munich, Germany nikolas.wilhelm@tum.de

[3]Maximilian Karl and Patrick van der Smagt are with the Volkswagen Group, Machine Learning Research Lab, 80805 Munich, Germany karlma@argmax.ai

[4]Hannes Höppner is with the Berliner Hochschule für Technik, Humanoid Robotics Laboratory, 13353 Berlin, Germany karlma@argmax.ai

† These authors have contributed equally to this work and share senior authorship.

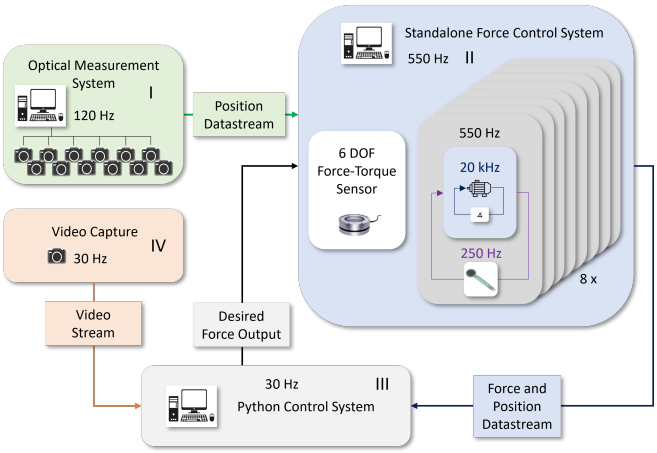

Fig. 1. Schematic representation of the test bench, featuring an optical measuring system (I), eight force-controlled motors (II) governed by a python control unit (III), and a video capture system (IV). An integrated 6 DOF force-torque sensor facilitates external load measurement.

1) We extend the testbench of force-controlled hand stimulation to eight independent motors.
2) We acquire external force–torque and motion data to analyze the resulting hand response to muscle actuation.
3) We apply and evaluate our test rig on a cadaver hand, performing complex tasks such as the pincer grip between the index finger and thumb.
4) A novel approach for biomechanically-derived modeling, advancing hand dynamics understanding, with a versatile robotic testbench suitable for diverse joint evaluations.

II. Material and Methods

A. Test Bench Architecture

The architecture of the test bench, depicted in Figure 1, integrates four primary components: the force control system, the optical measurement system (Optitrack©), the central control unit, and a video capture device.

The force control system integrates eight autonomous motors, each equipped with a strain gauge for force detection and an internal angle sensor. We employed 9225-160KV brushless motors, each boasting a maximum power of 1.6 kW. Using high-power pancake motors enables us to quickly and precisely maneuver and exert specific forces from standstill, which is crucial for fine-grained force control. Each motor's control is cascaded, with the motor's requisite force signal regulated in an external loop at 250 Hz. The force controller's output interfaces with the open-source Vedder electric velocity controller (VESC) [19], which offers precise field-oriented control (FOC) through an internal loop operating at 20 kHz. Additionally, a versatile 6 DOF force–torque sensor is incorporated into the system to measure the hand grip force.

Real-time data acquisition and force control are managed by an application developed on the Isaac SDK [20]. The optical measurement system, an OptiTrack© setup with six cameras, relays position and orientation data at 120 Hz to the force-control system.

The data stream, synchronized with force and position metrics, is relayed to the central control system. The video capture system, directly interfaced with the central control, delivers a video stream. While primarily used for evaluation, the video data can be augmented with AI-driven analyses, such as 3D hand reconstruction [21].

To simulate the pincer grip, each motor is individually regulated using signals characterized by a sine wave:

$$F_{\mathrm{des},i}(t) = a_i \cdot \sin(\omega_i t + \mathrm{off}_{\omega,i}) + \mathrm{off}_i, \qquad (1)$$

where off_i denotes the tendon's base tension, a_i represents the force oscillation amplitude, ω_i its frequency, and $\mathrm{off}_{\omega,i}$ the time offset for each motor i.

The test bench's key features encompass precise force control, synchronized sensor data, and real-time functionality, laying a solid groundwork for model-based control implementations.

TABLE I

Overview of the eight actuated tendons for the analysis of the interaction between thumb and index finger.

Finger	Tendon / Muscle	Function
Thumb	Extensor pollicis brevis	Extension
	Extensor pollicis longus	Extension
	Abductor pollicis longus	Abduction
	Flexor pollicis longus	Flexion
Index Finger	Extensor digitorum	Extension
	Extensor indicis	Extension
	Flexor digitorum superficialis	Flexion
	Flexor digitorum profundus	Flexion

B. Hand and Tendon Preparation

After obtaining approval from the local research ethics committee (699/21 S-SR), frozen human cadaver right hands with forearm of a 34 year old woman as well as a 72 year old man were used, which were obtained from Science Care, USA. Each thawed specimen was prepared by an experienced surgeon. 8 tendons of the thumb and index finger responsible for the pincer grip were identified and anatomically dissected. Table I shows a listing of the tendons with their function.

Each tendon was looped proximally to the flexor and extensor retinaculum at the wrist with stretch-free cords (LIROS DC 60 Dyneema®) to ensure physiological force application and not to influence the friction coefficient of the tendons (Fig. 2 a). The associated muscle and interfering soft tissue were removed.

Five custom SLA 3D-printed navigation trackers were fixed to the finger bones for position detection using an optical navigation system. These were screwed into a bicortical 3 mm hole with a conical thread in the corresponding bone and fixed with fast-curing epoxy resin (Pattex®).The trackers were attached to the distal phalanx and os metacarpale of the thumb and to the distal and proximal phalanx and os metacarpale of the index finger. The final tracker was used to track the positioning of the force-torque sensor. Care was

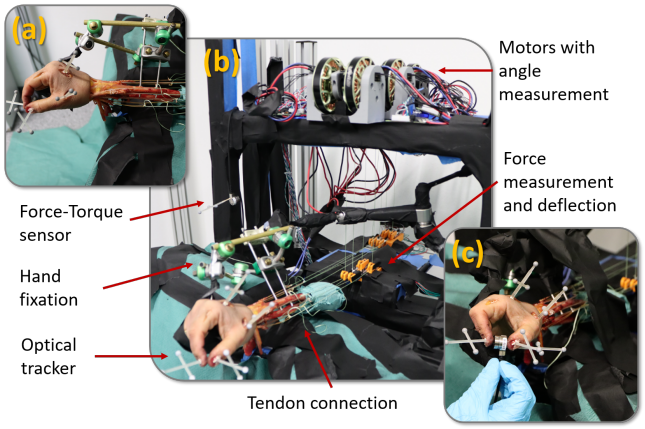

Fig. 2. Illustration of the test rig and setup: (a) Depicts the precise fixation of the cadaver hand to the test stand; (b) Provides an in-depth view of the overall test configuration; (c) Demonstrates the execution of the pincer grip, highlighting the integrated force-torque measurement with a mobile sensor strategically positioned between the index finger and thumb.

taken to ensure that the trackers do not interfere with each other in different positions.

The prepared hand was secured in the testing system using an external fixator (Hoffmann® II Compact™ MRI-Stryker) to maintain a stable intrinsic plus position, with two 4mm pins grasping the radial bone and one 3 mm pin placed in the metacarpal III shaft. Thin-layer computed tomography (CT) scans (Harmony, Siemens) were acquired to obtain data for bone segmentation and hand modeling.

When attaching the specimen to the test bench, the anatomical alignment of tendons and clear visibility of the tracker were ensured (Fig. 2 b). Throughout testing, the hand and tendons were periodically moistened to mitigate physiologic tissue alteration.

C. Datastream

Given the complex array of variables measured by the test stand, a more detailed explanation is warranted. An overview of the recorded signals, captured at specific points in time, can be found in Table II. This table offers a comprehensive breakdown, facilitating a clearer understanding of the data collection process. The setup consists of five rigid bodies tracked by OptiTrack© and providing the position, quaternion as well as the corresponding Cartesian and angular velocities for each time step. The tracked objects are the fingertip of index finger and thumb, as well as the corresponding bases and the force torque sensor. Further the force torque sensor provides forces and torques and the analog sensors connected to each tendon provide the respective force and force derivative for this tendon, resulting in a total of 95 signals per time step.

D. Workflow

The workflow for successful testing, illustrated in Figure 3, begins with the preparation of trackers and tendons for the cadaver hand, followed by computed tomography (CT) imaging and segmentation to accurately determine hand

TABLE II

SUMMARY OF RECORDED SIGNALS FROM THE TEST RIG, GROUPED BY SENSOR TYPE. THE TABLE DETAILS MEASUREMENTS OF POSITION, ORIENTATION, FORCES, TORQUES, AND DERIVATIVES FOR OPTITRACK© BODY, FORCE TORQUE SENSOR, AND ANALOG SENSOR CATEGORIES. TOTALS AT THE BOTTOM INDICATE THE NUMBER OF SIGNALS AND SENSORS FOR EACH.

Sensor Type	OptiTrack© Body	Force Torque Sensor	Actuation Sensors
Position	x, y, z	-	-
Orientation	q_w, q_x, q_x, q_z	-	-
Motor Angle	-	-	α
Forces	-	f_x, f_y, f_z	f
Torques	-	m_x, m_y, m_z	-
Derivatives	$\delta x, \delta y, \delta z$ $\delta\alpha, \delta\beta, \delta\gamma$	-	δf
num. signals	13	6	3
num. sensors	5	1	8
$\sum$ signals	65	6	24

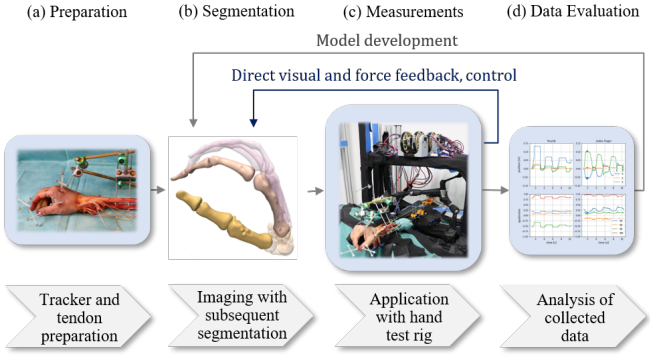

Fig. 3. Illustration of the test workflow: (a) preparation of tendons and trackers; (b) imaging and subsequent segmentation; (c) main testing on the test rig; (d) data evaluation and optimization of control parameters.

anatomy and tracker positions relative to finger bones. After the initial hand preparation, CT scans with installed trackers are acquired. Finger bones and corresponding trackers are segmented using a 3D slicer [22], enabling accurate determination of hand anatomy and tracker positions. The hand is then applied to the test rig, tendons are matched to their corresponding motors, and collected data is used for evaluation, model enhancement, and control optimization.

E. Kinematic Orientation

To determine the orientations of all rigid bodies at each timestep t, a systematic kinematic process must be conducted. Initially, the relationship between the rigid bodies and their corresponding trackers must be established. This can be accomplished by segmenting the rigid bodies from the CT and identifying the marker positions of each tracker within the CT system. Since the OptiTrack© system facilitates the exportation of marker positions for each registered tracker, two sets of points are obtained for every tracker—one defined in the CT system, and the other in the OptiTrack© base system. By employing the Kabsch algorithm [23], the transformation matrix from the CT system to the OptiTrack© base system, denoted as $T^{b_i}_{\text{opt,ct}}$, is obtained for each rigid

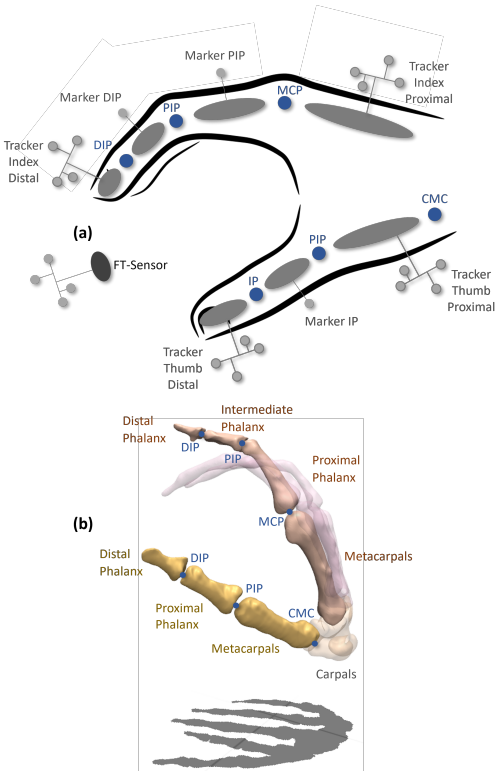

Fig. 4. (a) Displays all trackers used for accurate finger joint angle measurement in grey and the corresponding joint positions, highlighted in blue. (b) Presents the hand segmentation from the CT scan, with labels for all essential rigid bodies to analyze movement dynamics.

body b_i. A comprehensive representation of all required rigid bodies and markers is illustrated in Figure 4. Using the four provided rigid body trackers from Figure 4(a) we can calculate the transformation of each rigid body with a tracker at each timestep t using the measurement of the rigid body with respect to the OptiTrack© base system $T_{\text{opt},b_i}(t)$.

$$T^{b_i}_{\text{opt,ct}}(t) = T_{\text{opt},b_i}(t) \cdot T_{b_i,\text{ct}} \tag{2}$$

F. Kinematic Optimization for Undefined Rigid Bodies

Now that each rigid body with a corresponding tracker is defined for each timestep t, the task remains to identify the positions of the undefined bodies. Simplifying the task, the use of an external fixation allows us to safely assume that the metacarpal phalange of the index finger is affixed to the carpals of the hand, hence forming a rigid-body system. However, the positioning of the proximal and intermediate phalanges of the index finger, and the proximal phalange of the thumb, remains undetermined. To resolve this, a direct kinematic optimization is conducted using additional information from the CT scan: By defining the axis positions between each rigid body (IP, PIP, and CMC for the thumb, and DIP, PIP, and MCP for the index finger), we can articulate a rigid body kinematics relation for the undefined bodies.

For the thumb, the IP axis is repositioned using the distal thumb tracker (Figure 4(a)), and the PIP axis is defined using the proximal thumb tracker. As each axis is identified by two points from the CT scan, the Kabsch algorithm [23] can be used (requiring a minimum of three points) to pinpoint the final positioning of the proximal phalanx.

The index finger follows a similar strategy, allowing for the definition of the DIP and MCP axis points in the CT system with the available tracker data. However, with two undefined rigid bodies (the intermediate and proximal phalanges), an iterative process is proposed to finalize their positioning. Using the positioning of the unknown bodies from the CT scan, an initial solution is obtained by assuming a rigid body relation between the respective closest tracker body and the unknown rigid body. Next, the PIP axis position is updated according to this initial solution. With all required axes defined, an iterative update of the unknown rigid bodies is performed using the axis positions of the DIP and PIP for the intermediate phalanx, and the MCP and PIP for the proximal phalanx. Following each update, the PIP axis positioning is accordingly adjusted, with the MCP and DIP axes kept fixed. This iterative process ensures convergence on the accurate positioning of all rigid bodies of the index finger.

G. Calculation of Joint Angles in Phalanges

In the study, joint angles, except for the CMC joint, were systematically calculated using vectors for each phalanx, extending from the proximal joint to either the distal joint or fingertip, with additional points defined for the thumb and index finger.

The angles between adjacent phalanges were determined using standard vector methods. Specifically, for two vectors $\mathbf{v}_1$ and $\mathbf{v}_2$ representing the positions of the joints, the angle α between them was calculated using the formula:

$$\alpha = \arccos\left(\frac{\mathbf{v}_1 \cdot \mathbf{v}_2}{|\mathbf{v}_1| \cdot |\mathbf{v}_2|}\right) \tag{3}$$

where $\mathbf{v}_1 \cdot \mathbf{v}_2$ is the dot product of the vectors, and $|\mathbf{v}_1|$ and $|\mathbf{v}_2|$ are their magnitudes. This method was applied consistently across all joints, except for the CMC joint. For the CMC joint, which exhibited two-axis movement in testing, flexion and abduction were calculated using the vector of the metacarpal phalanx.

The resulting angles represent the phalanx's deviation from its default position, with the axis of abduction derived as the cross product of the axis of flexion and the vector pointing from the CMC to MCP joint. Shadow points on a plane defined by these axes were computed, and vectors to these points were used to precisely determine the flexion and abduction.

III. Results

This research sought to explore the proficiency of a test-bench setup in mimicking and quantifying the motions and forces characteristic of a human hand during a pincer grip action. Experiments utilized two hand specimens: a 34-year-old female right hand and a 72-year-old male hand (approval by local research ethics committee 699/21 S-SR). Due to tracking challenges encountered with the female specimen,

the emphasis was primarily placed on the male hand. A comprehensive dataset of the results can be accessed from the accompanying GitHub repository: `https://github.com/NikonPic/PhoenixHand`. These findings stem from two core actuation techniques: robotic and manual.

A. Robotic Actuation

The results from the experimental run, obtained through the application of motor-controlled forces, are presented in Figure 5. Each motor was programmed to follow an individual sinusoidal force trajectory, applying a specific force to its associated tendon. By iteratively optimizing each motor's trajectory parameters, a pincer grip was achieved using the given setup. Using the CT segmentation and tracking data from OptiTrack, a distinct correlation between tendon forces and the resultant finger movements—represented by the joint angles (as seen in Figure 5, top row)—is evident. However, the finger movement wasn't entirely physiologic. There were notable fluctuations in force control, evident in the force curves for the flexor pollicis longus (thumb) and the flexor profundus (index finger), as shown in the middle row of Figure 5. Moreover, the joint angles were suboptimal, with the MCP joint of the index finger being hyperextended (indicated by its negative value) and noticeable control instability in the IP joint of the thumb during motion.

B. Evaluation of Pincer Grip Force

In evaluating the performance of the tendon actuation, it is essential to consider the effectiveness of the resultant pincer grip force. For this purpose, an external force-torque sensor was strategically positioned between the fingertips, tasked with gauging the contact force during the grip. Figure 6 provides a comprehensive visual representation of the grip force results. The presented testbench was successful at performing the pincer grip with measurable contact forces. Quantitatively, the robotic actuation produced a force of 0.79 ± 0.09 N (mean ± standard deviation).

IV. Discussion

Our study, focused on replicating the motions and forces of a human hand during a pincer grip action, employed two hand specimens: a 34-year-old female right hand and a 72-year-old male right hand. Due to challenges with the female specimen, emphasis was placed on the male hand. Force evaluation, using an external force–torque sensor, revealed a pincer grip force of 0.79 ± 0.09 N for robotic actuation.

A. Advancements in Robotic Hand Actuation Research

The dynamic grasping capabilities demonstrated by soft drones with tendon-actuated grippers highlight the potential of soft robotics in aggressive grasping scenarios [24]. This evolution in the field underscores the importance of our research direction, which diverges from the mainstream by emphasizing the biomechanics of the human hand.

While many studies, such as [25], [26], and [27], are constrained by the number of motors and often limit actuation to a single finger, our research broadens the horizon. The tendency of some studies to lean towards simulation models often results in a sacrifice of comprehensive real-world data. This leaves the intricate relationship between muscle activation, movement, and the resultant force exerted by the finger largely uncharted.

Our research, however, distinguishes itself by covering a wider data collection spectrum. We have addressed prevalent gaps in the field, such as the omission of resultant finger grip forces [14] and the lack of motion tracking [28]. The use of cadavers in our methodology allows for more accurate measurements, standing in contrast to studies that rely on estimations [29]. Furthermore, our approach ensures a comprehensive and dynamic evaluation of tendon forces, setting it apart from methodologies like [28] that do not fully assess dynamic forces across all tendons.

B. Biomechanical Insights and Implications for Robotic and Prosthetic Design

The results of our experiments elucidate the biomechanics of the human hand. A significant observation was the discrepancy in forces produced by robotic and manual actuation. This difference may be attributed to the mechanical limitations of robotic actuators, which may not fully replicate the intricate biomechanical properties of human muscles. Additionally, the control algorithms governing robotic actuation might not capture the dynamic adjustments made by the human brain during manual actuation. The viscoelastic properties of human tendons, which change under different rates and durations of loading, might also contribute to the observed variations in force output.

Our research bridges human hand biomechanics with robotic, prosthetic, and rehabilitation technology design, aiming not to replicate the human hand's complexity but to abstract functional principles for enhanced adaptability and intuitiveness. Insights into the non-linear tendon force and grip strength relationship inform control algorithms for more natural robotic grip patterns. In prosthetics, these principles can improve dexterity and user integration, while in rehabilitation robotics, they enable more accurate human movement simulation for effective therapy. Furthermore, understanding hand mechanics fosters safer, more intuitive human-robot interactions, emphasizing the utility of biomechanical insights beyond mere replication towards innovative, user-centric applications.

C. Limitations

Our study, while offering valuable insights into the biomechanics of the human hand, encountered several challenges. The optical trackers, pivotal for data acquisition, occasionally experienced signal loss, notably compromising the evaluation of the initial female hand specimen. As testing progressed, the biomechanical properties, especially viscoelastic characteristics, of the cadaveric specimens underwent alterations, a phenomenon akin to mummification, which could influence the hand's response to actuation.

The determination of joint angles, integral to our analysis, presented potential inaccuracies. The reliance on manual

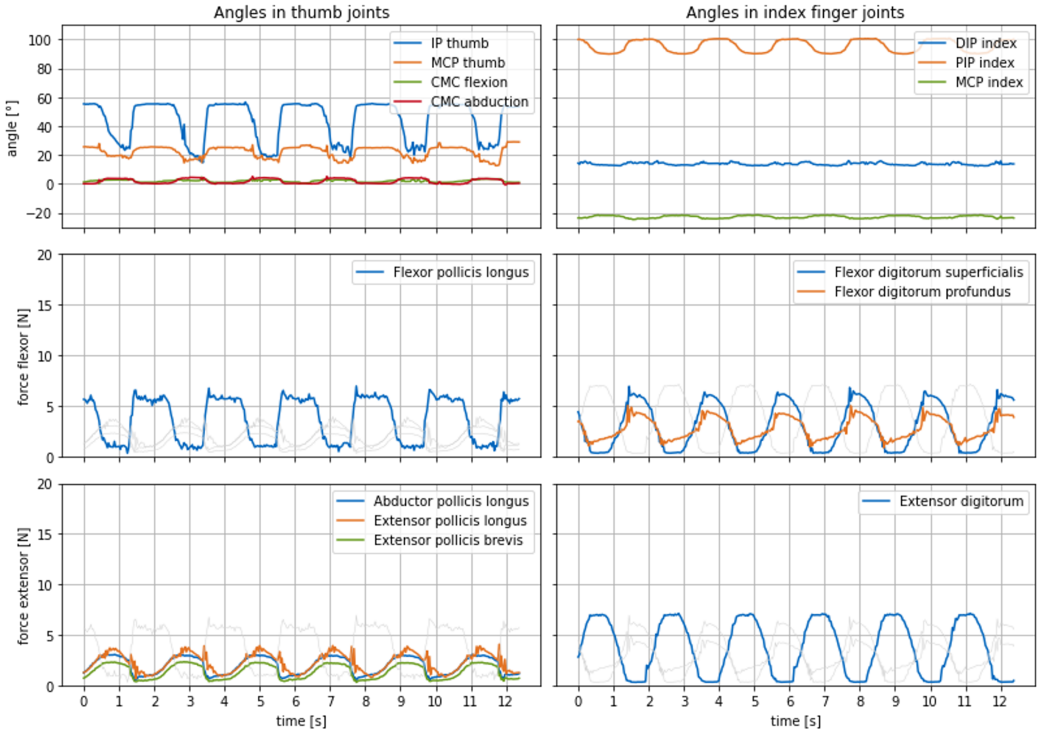

Fig. 5. Results from hand testing for the male hand, depicting thumb (left) and index finger (right) movements during **robotic** actuation. The top row displays joint angles, while the middle and bottom rows present forces from the corresponding tendons.

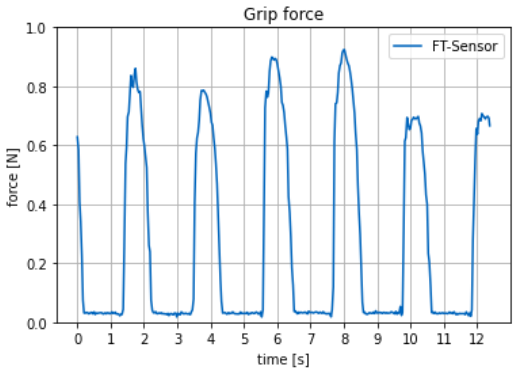

Fig. 6. Pincer Grip Force Measurements: This illustration depicts the force exerted during a pincer grip, as recorded by a force-torque sensor positioned between the tips of the index finger and thumb.

identification of joint positions for optimizing body positioning introduces variability and potential error into the measurements. Environmental factors, such as humidity and temperature, even with controlled conditions, might have subtly influenced the tissue properties, further affecting results. Additionally, the diversity of our hand specimens was limited, potentially constraining the generalizability of our findings. Factors like age, prior hand usage, and medical history can significantly influence hand biomechanics, and our selected specimens might not encompass the full variability of these parameters.

V. Conclusion

In this study, we delved deep into the biomechanics of the human hand, with a special emphasis on the intricate relationship between tendon forces and grip strength. Our interdisciplinary approach, which seamlessly integrated principles from both robotics and biomechanics, led to the successful evaluation of a testbench that stands out in its size and complexity of measurement. Notably, our setup is pioneering in its comprehensive nature, distinguishing itself from other studies that often limit the number of actuators, rely heavily on simulations, or omit real-world tests. Moreover, our use of external tracking further elevates the precision and reliability of our findings.

The pincer grip, executed effectively through both manual and robotic actuation of the eight motors, underscores the robustness and versatility of our experimental framework. Our results not only align with but also enhance the existing body of literature, addressing and filling notable gaps in data collection methodologies and their real-world applicability. The rich data we've gathered, capturing the subtle and complex mechanics of the human hand, lays a robust groundwork essential for future modeling endeavors.

As the link between biomechanics and robotics continues to grow, the findings from this study can serve as foundational knowledge to guide future research and innovation in the development of advanced biomechanic simulations of the human hand.

REFERENCES

[1] J M Landsmeer. Anatomical and functional investigations on the articulation of the human fingers. *Acta Anat Suppl (Basel)*, 25(24):1–69, 1955.

[2] N K Fowler and A C Nicol. Interphalangeal joint and tendon forces: normal model and biomechanical consequences of surgical reconstruction. *J Biomech*, 33(9):1055–1062, September 2000.

[3] Scott F M Duncan, Caitlin E Saracevic, and Ryosuke Kakinoki. Biomechanics of the hand. *Hand Clin*, 29(4):483–492, October 2013.

[4] Benjamin I Binder-Markey and Wendy M Murray. Incorporating the length-dependent passive-force generating muscle properties of the extrinsic finger muscles into a wrist and finger biomechanical musculoskeletal model. *J Biomech*, 61:250–257, June 2017.

[5] M Mirakhorlo, N Van Beek, M Wesseling, H Maas, H E J Veeger, and I Jonkers. A musculoskeletal model of the hand and wrist: model definition and evaluation. *Comput Methods Biomech Biomed Engin*, 21(9):548–557, September 2018.

[6] Lucas Engelhardt, Maximilian Melzner, Linda Havelkova, Pavel Fiala, Patrik Christen, Sebastian Dendorfer, and Ulrich Simon. A new musculoskeletal AnyBody™ detailed hand model. *Comput Methods Biomech Biomed Engin*, pages 1–11, December 2020.

[7] Alexander Synek, Marcus Settles, and Georg Stillfried. Multi-body simulation of a human thumb joint by sliding surfaces. In *2012 4th IEEE RAS and EMBS International Conference on Biomedical Robotics and Biomechatronics (BioRob)*, pages 379–384, 2012.

[8] Aude Billard and Danica Kragic. Trends and challenges in robot manipulation. *Science*, 364(6446), June 2019.

[9] Zhe Xu and Emanuel Todorov. Design of a highly biomimetic anthropomorphic robotic hand towards artificial limb regeneration. In *2016 IEEE International Conference on Robotics and Automation (ICRA)*, pages 3485–3492, 2016.

[10] Kazuki Mitsui, Ryuta Ozawa, and Toshiyuki Kou. An under-actuated robotic hand for multiple grasps. In *2013 IEEE/RSJ International Conference on Intelligent Robots and Systems*. IEEE, November 2013.

[11] Whitney Crooks, Gabrielle Vukasin, Maeve O'Sullivan, William Messner, and Chris Rogers. Fin ray® effect inspired soft robotic gripper: From the RoboSoft grand challenge toward optimization. *Frontiers in Robotics and AI*, 3, November 2016.

[12] Dan Hu, David Howard, and Lei Ren. Biomechanical analysis of the human finger extensor mechanism during isometric pressing. *PLoS ONE*, 9(4):e94533, April 2014.

[13] Maximilian Melzner, Lucas Engelhardt, Ulrich Simon, and Sebastian Dendorfer. Electromyography-Based validation of a musculoskeletal hand model. *J Biomech Eng*, 144(2), February 2022.

[14] Ashish D. Nimbarte, Rodrigo Kaz, and Zong-Ming Li. Finger joint motion generated by individual extrinsic muscles: A cadaveric study. *Journal of Orthopaedic Surgery and Research*, 3(1), July 2008.

[15] Joonho Chang, Andris Freivalds, Neil A Sharkey, Yong-Ku Kong, H Mike Kim, Kiseok Sung, Dae-Min Kim, and Kihyo Jung. Investigation of index finger triggering force using a cadaver experiment: Effects of trigger grip span, contact location, and internal tendon force. *Appl Ergon*, 65:183–190, July 2017.

[16] Angélica Vargas, Karla Chiapas-Gasca, Cristina Hernández-Díaz, Juan J. Canoso, Miguel Ángel Saavedra, José Eduardo Navarro-Zarza, Pablo Villaseñor-Ovies, and Robert A. Kalish. Clinical anatomy of the hand. *Reumatología Clínica*, 8:25–32, December 2012.

[17] Ming-Jin Liu, Cai-Hua Xiong, and Di Hu. Assessing the manipulative potentials of monkeys, apes and humans from hand proportions: implications for hand evolution. *Proceedings of the Royal Society B: Biological Sciences*, 283(1843):20161923, November 2016.

[18] Arend F Bos, Koenraad N J A Van Braeckel, Marrit M Hitzert, Jozien C Tanis, and Elise Roze. Development of fine motor skills in preterm infants. *Developmental Medicine Child Neurology*, 55:1–4, November 2013.

[19] Benjamin Vedder. VESC - Open Source ESC, 2022. Accessed: 2023-04-17.

[20] NVIDIA. Isaac sdk, 2022. Accessed: 2023-04-17.

[21] Xingyu Chen, Yufeng Liu, Dong Yajiao, Xiong Zhang, Chongyang Ma, Yanmin Xiong, Yuan Zhang, and Xiaoyan Guo. Mobrecon: Mobile-friendly hand mesh reconstruction from monocular image. *arXiv:2112.02753*, 2021.

[22] Andriy Fedorov, Reinhard Beichel, Jayashree Kalpathy-Cramer, Julien Finet, Jean-Christophe Fillion-Robin, Sonia Pujol, Christian Bauer, Dominique Jennings, Fiona Fennessy, Milan Sonka, John Buatti, Stephen Aylward, James V. Miller, Steve Pieper, and Ron Kikinis. 3d slicer as an image computing platform for the quantitative imaging network. *Magnetic Resonance Imaging*, 30(9):1323–1341, November 2012.

[23] Jim Lawrence, Javier Bernal, and Christoph Witzgall. A purely algebraic justification of the kabsch-umeyama algorithm. *Journal of Research of the National Institute of Standards and Technology*, 124, October 2019.

[24] Joshua Fishman, Samuel Ubellacker, Nathan Hughes, and Luca Carlone. Dynamic grasping with a "soft" drone: From theory to practice. In *2021 IEEE/RSJ International Conference on Intelligent Robots and Systems (IROS)*. IEEE, September 2021.

[25] Andreas Schweizer and Robert Hudek. Kinetics of crimp and slope grip in rock climbing. *Journal of Applied Biomechanics*, 27(2):116 – 121, 2011.

[26] Kim Seng Fok and Siaw Meng Chou. Development of a finger biomechanical model and its considerations. *Journal of Biomechanics*, 43(4):701–713, 2010.

[27] Benjamin I. Binder-Markey and Wendy M. Murray. Incorporating the length-dependent passive-force generating muscle properties of the extrinsic finger muscles into a wrist and finger biomechanical musculoskeletal model. *Journal of Biomechanics*, 61:250–257, 2017.

[28] Joonho Chang, Andris Freivalds, Neil A. Sharkey, Yong-Ku Kong, H. Mike Kim, Kiseok Sung, Dae-Min Kim, and Kihyo Jung. Investigation of index finger triggering force using a cadaver experiment: Effects of trigger grip span, contact location, and internal tendon force. *Applied Ergonomics*, 65:183–190, 2017.

[29] Dan Hu, David Howard, and Lei Ren. Biomechanical analysis of the human finger extensor mechanism during isometric pressing. *PLOS ONE*, 9(4):1–11, 04 2014.